Published in final edited form as:

ACS Appl Mater Interfaces. 2020 April 08; 12(14): 16006–16017. doi:10.1021/acsami.9b22964.

Injectable MMP-Responsive Nanotube-Modified Gelatin Hydrogel for Dental Infection Ablation

Juliana S. Ribeiro

Department of Cariology, Restorative Sciences and Endodontics, School of Dentistry, University of Michigan, Ann Arbor, Michigan 48109, United States;

Department of Restorative Dentistry, School of Dentistry, Federal University of Pelotas, Pelotas, Rio Grande do Sul 96010-610, Brazil

Ester A. F. Bordini

Department of Cariology, Restorative Sciences and Endodontics, School of Dentistry, University of Michigan, Ann Arbor, Michigan 48109, United States;

Department of Dental Materials and Prosthodontics, School of Dentistry, São Paulo State University, Araraquara, São Paulo 01049-010, Brazil

Jessica A. Ferreira,

Department of Cariology, Restorative Sciences and Endodontics, School of Dentistry, University of Michigan, Ann Arbor, Michigan 48109, United States

Ling Mei,

Department of Pharmaceutical Sciences, College of Pharmacy and Biointerfaces Institute, University of Michigan, Ann Arbor, Michigan 48109, United States

Nileshkumar Dubey,

Department of Cariology, Restorative Sciences and Endodontics, School of Dentistry, University of Michigan, Ann Arbor, Michigan 48109, United States

J. Christopher Fenno,

Department of Biologic and Materials Sciences & Prosthodontics, School of Dentistry, University of Michigan, Ann Arbor, Michigan 48109, United States

Evandro Piva,

Department of Restorative Dentistry, School of Dentistry, Federal University of Pelotas, Pelotas, Rio Grande do Sul 96010-610, Brazil

Rafael G. Lund,

Department of Restorative Dentistry, School of Dentistry, Federal University of Pelotas, Pelotas, Rio Grande do Sul 96010-610, Brazil;

Anna Schwendeman,

Corresponding Author: Marco C. Bottino –*Department of Cariology, Restorative Sciences and Endodontics, School of Dentistry, University of Michigan, Ann Arbor, Michigan 48109, United States;* Phone: +1-734.763.2206; mbottino@umich.edu; Fax: +1-734.936.1597.

The authors declare no competing financial interest.

Department of Pharmaceutical Sciences, College of Pharmacy and Biointerfaces Institute, University of Michigan, Ann Arbor, Michigan 48109, United States;

Marco C. Bottino
Department of Cariology, Restorative Sciences and Endodontics, School of Dentistry, University of Michigan, Ann Arbor, Michigan 48109, United States;

Abstract

A photocrosslinkable gelatin methacryloyl (GelMA) hydrogel has been widely examined in regenerative engineering because of its good cell-tissue affinity and degradability in the presence of matrix metalloproteinases. A halloysite aluminosilicate nanotube (HNT) is a known reservoir for the loading and sustained delivery of therapeutics. Here, we formulate injectable chlorhexidine (CHX)-loaded nanotube-modified GelMA hydrogel that is cytocompatible and biodegradable and provides sustained release of CHX for infection ablation while displaying good biocompatibility. The effects of HNTs and CHX on hydrogel degradability and mechanical properties, as well as on the kinetics of CHX release, and on the antimicrobial efficacy against oral pathogens were systematically assessed. Cytocompatibility in stem cells from human exfoliated deciduous teeth and inflammatory response *in vivo* using a subcutaneous rat model were determined. Our hydrogel system, that is, (CHX)-loaded nanotube-modified GelMA showed minimum localized inflammatory responses, supporting its ability for drug delivery applications. Moreover, we showed that the incorporation of CHX-loaded nanotubes reduces the mechanical properties, increases the swelling ratio, and diminishes the degradation rate of the hydrogels. Importantly, the presence of CHX-loaded nanotubes inhibits bacterial growth with minimal cell toxicity. Our findings provide a new strategy to modify GelMA hydrogel with chlorhexidine-loaded nanotubes for clinical use as an injectable drug delivery strategy for dental infection ablation.

Graphical Abstract

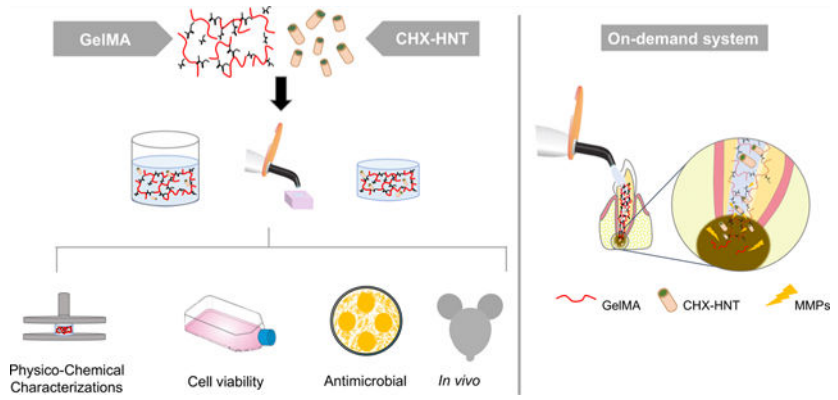

Keywords

drug delivery; hydrogel; infection; endodontics; dentistry; matrix metalloproteinases

INTRODUCTION

Dental caries are the most common chronic disease among children and young adults aged 6–19 years.[1] Etiologically speaking, caries is a time-dependent multifactorial infectious disease, which, if not properly managed, may lead to pulp tissue necrosis and consequential endodontic therapy.[2] Appraisals from the American Association of Endodontists indicate that nearly 16 million patients undergo root canal treatment every year in a procedure that involves surgical removal of the necrotic pulp tissue, followed by disinfection, mechanical instrumentation of the root canal, and final sealing with a thermoplastic material prior to tooth restoration.[3]

The microbial population in endodontic infections changes as the infection progresses. First, the infection is characterized mostly by the presence of facultative microbes.[4,5] Over time, an environment-favoring anaerobic growth is established, both with the decline in oxygen levels because of bacterial metabolism and the lessening of blood flow because of tissue necrosis.[6] For example, *Porphyromonas gingivalis*, an obligatory anaerobic Gram-negative microbe, has been linked with endodontic infections, especially in apical periodontitis.[6] Of note, in addition to the most common virulence factors such as lipopolysaccharides, *P. gingivalis* proteinases (collagenases) have been shown to play a key role in its pathogenesis mechanism.[7,8]

Clinically speaking, the root canal anatomy is highly complex, and thus the mechanical removal of tissue remnants, biofilm, and infected dentin cannot always guarantee a bacteria-free niche.[9] As a result, infected tissues can be left behind, where microorganisms can grow and proliferate.[10] Collectively, the anatomical challenges, as well as the presence of clinical signs and symptoms, strongly support the indication of a multiple-visit therapy and employment of intracanal medications.[11] Although calcium hydroxide [$Ca(OH_2)$] has been used clinically as an interappointment medication, research shows that it may not be entirely effective against *Enterococcus faecalis* and *Candida albicans*. Instead, chlorhexidine digluconate (CHX) has been suggested based on its ability to ablate periapical inflammation.[12,13] Unfortunately, a growing body of research suggests dose-dependent toxicity;[14,15] thus, underscoring the need to develop a delivery system to promote the controllable release of low, yet potent, antimicrobial doses of CHX. In this way, advances in the use of aluminosilicate clay nanotubes (Halloysite, HNT) as a reservoir for the loading and sustained delivery of therapeutics, reported by our group[16,17] and others,[18,19] present new prospects in designing injectable and degradable nanotube-modified hydrogels aimed at ablating endodontic infection with minimal or no adverse reactions. In detail, as previously reported, the modification of polymeric fibers with tetracycline (TCH)-loaded nanotubes led to sustained and controlled release, as opposed to the burst liberation observed when TCH was directly added into the fibers.[20]

Gelatin methacryloyl (GelMA) is a biocompatible and biodegradable photopolymerizable hydrogel that originated from the modification of amine-containing side groups of gelatin (Gel) with methacrylamide and methacrylate groups.[21,22] GelMA has many properties useful in biological interactions, including its hydrophilicity, integrin-binding motifs, and matrix metalloproteinase (MMP) degradation sites.[23] Similar to other reported hydrogels,

when considering its use in drug delivery, GelMA can be efficiently mixed with a wide array of additives, such as but not limited to nanotubes and biomolecules.[24] Of note and highly relevant to the proposed work, during periapical pathology development, after endodontic therapy, persistent infections have been associated with increased levels of MMP (MMP-1, MMP-2, MMP-8, and MMP-9) in the periapical area.[25,26] Thus, we postulate that a photopolymerizable GelMA could be successfully tuned to function as an on-demand depot of CHX that would be triggered by the hydrogel exposure to high levels of MMPs, thus releasing the therapeutic agent once apical periodontitis has been established. To the best of our knowledge, the present study is the first to report on the synthesis and clinical potential of an on-demand (MMP-responsive) injectable, biodegradable, and biocompatible nanotube-modified GelMA hydrogel system for delivering CHX intracanal as a suitable strategy for dental infection ablation.

RESULTS AND DISCUSSION

Our findings suggest an on-demand (MMP-responsive) system for delivering CHX intracanal from an injectable, biodegradable, and biocompatible nanotube-modified hydrogel. A delivery mechanism, primarily based on GelMA degradation successfully mediated by MMP presentation and subsequent liberation of antimicrobial potent and cytocompatible CHX concentration, is demonstrated.

Halloysite Nanotube Modification.

The morphological details (length 321–806 nm and diameter 50.2–108 nm) of the nanotubes are presented in Figure 1a,b. Of note, transmission electron microscopy (TEM) micrographs clearly display the lumen, which allowed for the loading of CHX. The Halloysite spectrum showed characteristic peaks at ~3696 cm^{-1} associated with Al_2-OH stretching. Additional peaks at ~1017 associated with the Si-O stretching and at ~911 associated with Al_2-OH bending can be seen (Figure 1c and inset Table). The spectra of H-C10% and H-C20% are derived from the modification with CHX. Peaks at 1643 and 1581 cm^{-1} are related to C=N stretching vibration. The peak at ~1529 cm^{-1} corresponds to the nitrogen-hydrogen bond in CHX supporting the HNT-CHX interaction.

CHX-Loaded Nanotube-Modified GelMA Hydrogels.

To appreciate the morphological features of the formulated hydrogels, cross-section scanning electron microscopy (SEM) micrographs were obtained. It is well-known that during freeze-drying, the porosity of the material can experience changes; thus, all samples were processed in the same fashion. As exhibited in Figure 2a, GelMA (without HNT) shows a highly porous structure with a pore size ranging from 40 to 143 μm. In contrast, SEM micrographs (Figure 2b) indicate that the incorporation of HNT into the GelMA did not change the uniform porous structure. More importantly, upon SEM inspection, HNT-modified hydrogels presented a textured surface, thus suggesting the presence of fairly well-distributed HNTs. Indeed, chemical analysis using energy-dispersive spectroscopy (EDS) further highlights the presence and homogeneous distribution of HNTs within the hydrogel matrix (Figure 2c,d). Notably, elemental mapping based on BSE-EDS analysis further confirms the chemical nature of the nanotubes by the presence of Si and Al (Figure 2e–h),

the major components of the HNTs.[27] It is well established that a 3D architecture with highly interconnected pores provides an advantageous environment for tissue regeneration, playing an important role in cell adhesion, migration, and proliferation. The obtained microstructure creates a suitable environment for cell penetration, supporting the rate of diffusion of oxygen and the uniform nutrient and waste exchange inside the hydrogels, allowing for and helping the deposition of extracellular matrix by the cells.[28,29]

Drug Release.

The release profiles of CHX from nanotube-modified GelMA hydrogels as a function of time are shown in Figure 3a,b. It is possible to observe a greater CHX release from H-C10% than H-C20%. It has been reported that sustained drug release may be because of the small size of HNTs, which confines drug diffusion. Noteworthy, although CHX-loaded HNTs were washed after loading, CHX can also be adsorbed on the external HNT surface. Although we did not show the loading efficiency (%) data, we anticipated that the CHX solutions at 10 and 20% would lead to ~19 and 29% loading efficiency, respectively, according to previously published work using a different but also cationic molecule of similar molecular weight (doxycycline M_w = 5054 g/mol; CHX M_w = 4444 g/mol). Moreover, within the first 24 h, the nanotube-modified hydrogels released between ~46% (1%H-C10%) and ~26% (2%H-C20%) of their total drug amount released over time. The mean drug amounts released from the 5%H-C10% and 5%H-C20% hydrogels were 6.5 and 5.3 μg/mL, respectively, after 24 h. This result may be attributed to the ability of the drug to intercalate in the lumen and be adsorbed on the external surface of the nanotubes. However, upon vacuum application, CHX may be pushed into the HNT lumen because of negative pressure, regardless of the charge of the materials affecting drug release. Regarding the decrease in CHX release upon increased HNT concentration, this might be explained by the specific binding affinity between CHX and the fairly large HNT surface area. Nonetheless, the reported amounts promoted significant bacterial growth inhibition of the pathogens tested. Sustained drug release may prolong the contact time of the drug with the microorganism leading the amount of drug released into the medium, reaching a level wherein the concentration could locally ablate the infection with minimal or no cell toxicity.[30]

Swelling and Degradation.

The swelling ratio was investigated to determine the hygroscopicity of the nanotube-modified hydrogels. The results indicated that the addition of HNTs directly affected the swelling properties. The CHX-loaded nanotube incorporation into GelMA absorbs higher amounts of water into the material structure that slightly enhances its swelling ratio (Figure 4a). However, no significant differences were found between H-C10% and H-C20%. This higher swelling ratio typically indicates a network structure with larger pores and higher interstitial volume available, which improves the degradability of the materials because of the formation of fewer cross-links.[31,32] It is desirable for a hydrogel to maintain specific amounts of water in its structure because this property is related to the nutritional supply of cells.[33]

Concerning the degradation profile of GelMA and the effect of the CHX loading via nanotube incorporation, we postulated that collagenase type I would mediate hydrogel degradation and thus CHX release. Knowing that GelMA hydrogels are MMP-sensitive, Figure 4b shows the complete degradation of the tested samples after 14 days. Statistical analysis revealed that HNT without CHX degraded faster than the groups modified with CHX-loaded nanotubes ($p = 0.05$). At 7 days, degradation of the groups with no added CHX was similar to groups modified with CHX at 10% and greater than the groups where CHX was added at 20%. On day 14, the non-CHX groups were completely degraded. At 21 days, no statistical differences were found among the remaining groups. In general, HNT-CHX incorporation significantly reduced the degradation rate of GelMA because of the presence of more chemical bonds formed among the hydrogel and the HNT-CHX, taking more time to be degraded by the MMP enzyme.[34] It has been related that the degradation speed of GelMA was inversely correlated with the degree of functionalization, the hydrogel concentration, and the amount of enzyme present.[35] Nonetheless, despite the groups showing rapid *in vitro* degradation, the actual degradation within the root canal may be slower, as it is a closed environment.[33] Thus, the hydrogel would be trapped in the canal space and mainly subjected to MMP action, such as in cases of recurrent apical periodontitis.[13]

Biomechanical Properties.

Previous studies aimed at strengthening hydrogels using inorganic nanoparticles (*e.g.*, hydroxyapatite, silicate, *etc.*) have reported the importance of optimizing particle concentration because a threshold limit, in terms of reinforcement, appears to exist, primarily because of particle agglomeration, which can act as a microstructural defect.[24] For example, the incorporation of minute amounts (up to 0.5%) of nanosilicates in GelMA led to a significant enhancement in mechanical properties; however, it is worth mentioning that nonstatistical differences were found between 0.05 and 0.5%. Hence, in the present work, the addition of HNTs (up to 5%) with or without loaded CHX did not promote significant biomechanical changes of GelMA (Figure 5a,b), except for 1%H-C10% and 1%H-C20%, which although statistically similar to unmodified GelMA, was not significant compared to most of the other nanotube-modified hydrogels. Taken together, the reported decrease in compressive modulus can be primarily attributed to the concentration of HNTs used.

Cytotoxicity.

Determining the *in vitro* cytotoxicity of the proposed hydrogel system is the key to validating its potential application as an on-demand intracanal drug delivery system for dental infection ablation. Here, we investigated the cytocompatibility of the hydrogels with human stem cells from exfoliated deciduous teeth (SHEDs). In comparison with the control (SHEDs cultured on the tissue culture plate), the number of surviving cells decreased after 24 h of exposure to the aliquots collected on day 3, for both concentrations (10 and 20%) of CHX-loaded nanotube-modified GelMA hydrogels (Figure 6). Nonetheless, the overall data showed an increase in cell viability above 70–80% for all groups when aliquots of 14, 21, and 28 days were tested. This might be explained by the fact that from day 3, a step-up in CHX release occurred, which agrees with the drug release data.

Screening CHX-Loaded Nanotube-Modified Hydrogels with the Best *In Vitro* Antimicrobial Properties.

Aiming to confirm the hypothesis that our proposed hydrogel possesses an on-demand drug delivery ability, agar diffusion assays were carried out with aliquots collected in two ways. Hydrogel samples of each group were placed in two different incubation media. As expected, for samples stored in PBS, the aliquots showed no bacterial inhibition for all groups in all-time points, thus supporting our hypothesis (MMP-responsive GelMA degradation). In the meantime, aliquots obtained through incubation in the on-demand challenge (1 U/mL collagenase type A in sterile PBS) led to noticeable antimicrobial action over 21 days against four oral pathogens (Figure 7). Noteworthy, the incorporation of CHX-loaded nanotubes (CHX at 10 and 20%) at 5 wt % led to greater inhibition zones against all microorganisms.

Direct Contact.

E. faecalis is Gram-positive bacteria known to be associated with secondary endodontic infection, and its persistence is credited with its capacity to colonize the root canal and resist treatment.[6] *E. faecalis* can occur singly, in pairs, or as short chains. They are small enough to proficiently invade and live within dentinal tubules and have the capacity to endure prolonged periods of starvation until an adequate nutritional supply becomes available.[36] Once the bacteria become available in the planktonic form inside dentinal tubules, it is critical to assess the antimicrobial effects of our GelMA-based hydrogels in a planktonic model. Taking into consideration the data collected in the agar diffusion assay, the following groups were tested, namely, 5%H-10%C and 5%H-20%C, as well as $Ca(OH)_2$ and pristine GelMA as positive and negative controls, respectively. Significant differences were noticed among the CHX-loaded nanotube-modified hydrogels (5%H-10%C and 5%H-20%C) and $Ca(OH)_2$ when compared to unmodified/pristine GelMA (Figure 8a).

Microcosm Biofilm.

It is important to highlight that the direct contact test evaluated the action of the medication against the planktonic form of the bacteria. The physiological properties of the same bacteria in the culture medium are markedly different when compared to the bacterial cells in biofilms that are protected by the biofilm-specific extracellular matrix.[37] It is well known that root canal infections are biofilm mediated and, according to the literature bacteria in biofilms, maybe 1000× times more resistant to antimicrobial agents and host defense mechanisms than their planktonic equivalents.[38] Therefore, to assess not only the antimicrobial activity against *E. faecalis* in a planktonic model but also the antimicrobial performance of our CHX-loaded nanotube-modified GelMA hydrogel in a more complex model, a microcosm biofilm model was used. As shown in Figure 8b, both the 5%H-C10% and 5%H-C20% groups led to the greatest biofilm inhibition, which was statistically different than the other groups. Notably, $Ca(OH)_2$ did not demonstrate significant action against the biofilm. In the SEM micrographs (Figure 8c–i), it is possible to note the presence of bacterial biofilm in the inner root walls of dentin slices of the unmodified GelMA, CHX-free nanotube-modified, and GelMA groups. However, in the CHX-loaded nanotube-modified GelMA hydrogels, a marked absence of bacteria on the dentin surface and inside

the dentinal tubules was noticed. Our data are in accordance with a previous study,[39] where the use of CHX in a drug delivery system was more effective against *E. faecalis* when compared to $Ca(OH)_2$. However, it is important to emphasize that the efficacy of the $Ca(OH)_2$ paste is associated with prolonged disinfection periods, at least 7 days.[40] There has been increasing concern about the insufficient antimicrobial efficacy of $Ca(OH)_2$ against *E. faecalis*, even after prolonged contact between the medication and root canal.[40] On the other hand, the most emblematic feature of CHX is that its positively charged molecules can be adsorbed by dentin, preventing microbial colonization as a result of its substantive antimicrobial activity.[41]

In Vivo Biocompatibility and Biodegradation.

As we know from the literature, *in vitro* and *in vivo* responses induced by biomaterials may be different *in vitro* and *in vivo*. Hence, subcutaneous implantation in rats was used for biocompatibility and biodegradation evaluation.[42] In this study, GelMA, 5%H, and 5%H-C10% hydrogels were evaluated after subcutaneous implantation in rats (Figure 9).

Representative images obtained after hematoxylin and eosin (H&E) staining of GelMA, 5%H, 5%H-C10%, and SHAM explants after 7 and 14 days *in vivo* are shown in Figure 10. Overall, no signs of host inflammatory responses were observed. At days 7 and 14, 5%H and 5%H-C10% hydrogels revealed minimal inflammatory cell infiltration, mainly being restricted to the borders of the hydrogels. The host cells that did infiltrate appear to be mononuclear cells (*e.g.*, macrophages, monocytes), as evidenced by cellular morphology. Ingrowth of blood vessels was observed at sparse locations around the borders of both GelMA, 5%H, and 5%H-C10% (yellow arrowheads) hydrogels at both time points, indicating material compatibility with angiogenesis. Additionally, no foreign-body giant cells were found in any of the evaluated groups. These results demonstrate the low immunogenicity of GelMA, regardless of the presence of nanotubes or CHX. The findings of this work are in agreement with previous studies that have shown that GelMA hydrogels did not exert cytotoxicity.[43]

Our histological data also illustrate specific details about hydrogel degradation process *in vivo*. As depicted in Figure 11, the GelMA hydrogel shows significant degradation at 7 days, with continuous resorption at 14 days. Meanwhile, the GelMA constructs were still present at the implantation site after 14 days. In contrast, the 5%H-C10% showed a slower degradation profile on days 7 and 14 compared to GelMA and 5%H counterparts, respectively. Collectively, the *in vivo* biodegradation results correlate well with those obtained *in vitro*, whereby the GelMA hydrogel degraded rapidly, with almost half of mass loss on day 14. Moreover, the data show that the presence of CHX-loaded nanotubes significantly reduced the degradation rate of GelMA, which can be attributed to the potential physical masking by HNTs of the sites of action for an enzymatic reaction. Our findings agree with similar work, where the presence of nanosilicates up to 0.5% (w/v) led to a significantly reduced degradation rate.

Results demonstrated that both *in vitro* and *in vivo* degradation rate of the formulated GelMA-based hydrogels were dependent on HNTs and CHX concentration. Overall, these results confirmed that composite hydrogels could be efficiently degraded *in vivo*, through

the simultaneous action of multiple phagocytes and interrelated degradation pathways.[44–48] Neutrophils and monocytes might be able to initially shape degradation via the release of hydrolytic enzymes (serine proteases). These compounds can modulate the degradation process, making it more or less vulnerable to the propagation of macrophage-driven degradation.[45] Of note, despite the groups showing rapid *in vitro* and *in vivo* biodegradation, the actual degradation within the root canal may be slower, as it is a closed environment. Nonetheless, although the site of implantation differed from the proposed clinical application, it is worth mentioning that the subcutaneous *in vivo* biocompatibility model performed herein had representative mechanisms and consequences of tissue-biomaterial interactions and is the most commonly used model able to provide an initial assessment of biomaterial compatibility with living tissues and degradation kinetics mediated by endogenous enzymatic mechanisms.

The main goal of the endodontic (root canal) treatment is to remove bacteria, virulence factors, and toxins in order to eradicate the inflammatory reaction in the apical area. Once the area is free of bacteria and its products, the inflammatory process and inflammatory cells slow down. Thus, we can infer that root canal treatment acts by reducing the active and latent forms of MMPs in root canal exudates and, in turn, the destruction of MMP-dependent inflammatory tissue.[49] Within this context, chlorhexidine has been used as an adjunct medication in periapical treatment,[39,50] particularly in situations where the root is not completely formed (open apex). In sum, we successfully engineered an on-demand intracanal drug delivery system based on the modification of GelMA with halloysite nanotubes loaded with chlorhexidine. Overall, we present strong evidence that our GelMA-based injectable drug delivery system would be clinically suitable for a number of therapeutic strategies, aiming at ablating infection, particularly prior to regeneration in cases of endodontic and periodontal applications.

CONCLUSIONS

In this study, we formulated injectable chlorhexidine (CHX)-loaded nanotube-modified GelMA hydrogel that is cytocompatible, biodegradable, and provides sustained release of CHX for dental infection ablation. Taking into consideration the lack of dental stem cell toxicity of the designed (CHX)-loaded nanotube-modified hydrogel system in addition to good biocompatibility and minimum localized inflammatory responses as determined by *in vivo* experiments, we can envisage that the proposed injectable GelMA-based hydrogels can be used for sustained intracanal drug delivery applications in endodontics. Nonetheless, further *in vivo* studies (periapical disease model), based on this proof-of-concept research, should be performed in order to enable the translation of the proposed drug delivery strategy to the clinics.

EXPERIMENTAL SECTION

Materials and Chemicals.

Aluminosilicate clay nanotubes (HNT, Halloysite, Dragonite HP) were obtained as a gift from Applied Minerals Inc. (New York, NY, USA). The TEM grid (Cu 200 mesh) was purchased from Structure Probe, Inc. (West Chester, PA, USA). Chlorhexidine digluconate

(20%) aqueous solution, type-A Gel (300 bloom) from porcine skin, methacrylic anhydride (MA), L-glutamine, brain heart infusion (BHI) broth, and agar were procured from Sigma-Aldrich (St. Louis, MO, USA). Dulbecco's phosphate-buffered saline (DPBS), alpha-modified Eagle's medium (α-MEM), fetal bovine serum (FBS), and penicillin-streptomycin were acquired from Gibco-Invitrogen (San Diego, CA, USA). Absolute-200 proof ethanol (Fisher Scientific, Waltham, MA, USA), lithium phenyl-2,4,6-trimethylbenzoylphosphinate (LAP L0290, TCI America, Portland, OR, USA), ethylenediamine tetra-acetic acid (EDTA; Inter-Med, Inc., Racine, WI, USA), collagenase type I (Hoffman-La Roche Ltd., Basel, Switzerland), and CellTiter 96 AQueous One Solution Reagent (Promega Corporation, Madison, WI, USA) were obtained from their respective manufacturers.

CHX Loading into Nanotubes.

To validate the morphological characteristics of Halloysite, TEM (JEM-2010, JEOL, Tokyo, Japan) was done. Briefly, 10 μL of an aqueous dispersion of sieved (<45 μm) HNTs was pipetted onto a holey carbon TEM grid, allowed to air-dry, and imaged at 100 kV.[16]

Chlorhexidine digluconate was used to prepare 10 and 20% CHX solutions (v/v) in distilled water for HNT loading, as previously established by our group.[16] The sieved HNTs (1.25 g) and 5 mL of the respective CHX solutions were centrifuged, vortexed for 20 s, and sonicated for 2 h. Then, the mixture was placed in a vacuum (25 in. Hg) chamber (Hi-Temp Vacuum, Thermo Scientific Inc.). After 1 h, the mixture was vortexed for 1 h, and the vacuum was reapplied. Finally, the HNT + CHX solutions were washed and centrifuged (3000 rpm) for 10 min and then stored at 37 °C for 7 days until completely dried. The dried mixture was once again sieved at 45 μm and dried prior to further use.[16] CHX-loaded HNTs were obtained (hereafter referred to as H-C10% and H-C20%, respectively). Fourier transform infrared spectroscopy in the attenuated total reflection mode (FTIR-ATR, Nicolet iS50, Thermo Fisher Scientific Inc.) was carried out to assess the presence of CHX. The spectra of pristine HNTs, CHX, and CHX-loaded nanotubes were collected in the 400–4000 cm^{-1} range with a resolution of 4 cm^{-1} (64 scans).

Gelatin Methacryloyl.

GelMA synthesis was carried out as described previously.[51,52] Briefly, on a heating plate at 50 °C, type-A Gel (10% w/v) was solubilized into DPBS. Next, 8 mL of MA was introduced dropwise into the Gel solution and allowed to react for 2 h under stirring conditions. To ensure the interruption of the reaction, an equal amount (8 mL) of DPBS was added at 40 °C. Finally, in order to remove salts and unreacted monomers, the mixture was dialyzed in deionized (DI) water using 12–14 kDa dialyze tubing at 45 ± 5 °C for 1 week, and the water was changed every 12 h. The prepared solution was frozen at −80 °C overnight, lyophilized (Labconco FreeZone 2.5 L, Labconco Corporation, Kansas City, MO, USA) for 7 days, and stored at −80 °C until further use.[23]

CHX-Loaded Nanotube-Modified GelMA Formulation and Characterization.

To create GelMA-based hydrogels, 0.6 g of GelMA was dissolved in 4 mL of DPBS at 50 °C. This was followed by the addition of 0.45 mg of the photoinitiator (LAP) at 50 °C under stirring (240 rpm) conditions, thus establishing the pure GelMA group (15% GelMA,

control). CHX-loaded nanotubes (H-C10% and H-C20%) at specified amounts (1, 2, and 5% w/v; hereafter referred as 1%H, 2%H, and 5%H) were mixed via magnetic stirring (240 rpm) for 2 h for dispersion into the GelMA solutions. Analogously, CHX-free nanotubes in the aforementioned amounts were also added to GelMA. To fabricate the GelMA and GelMA-modified samples for the various analyses reported, predetermined volumes ranging from 100 to 150 μL of the prepared solutions were placed in custom-made silicone molds (CutterSil Putty PLUS, Kulzer US, South Bend, IN, USA) and photocross-linked for 15 s with a curing LED light (Bluephase, Ivoclar Vivadent, Amherst, NY, USA) with a broadband spectrum of 385–515 nm. After cross-linking, the samples were removed from their molds.

The microstructures of GelMA and nanotube-modified GelMA hydrogels were evaluated by SEM (Tescan MIRA3 FEG-SEM, Tescan USA Inc., Warrendale, PA, USA). The pore morphology was analyzed in cylindrical-shaped (6 mm diameter × 10 mm thick) samples prepared as previously described. Prior to SEM imaging, samples (n = 3/group) were freeze-dried, cross-sectioned, and sputter-coated with Au-Pd. Elemental mapping was carried out using EDS by electron backscattered diffraction (EBSD) and an EDAX Hikari EBSD camera mounted on a scanning electron microscope to determine the chemical constituents.

Drug Release.

Ultra-performance liquid chromatography (UPLC) was used to investigate the release profile of CHX from the various CHX-loaded nanotube-modified GelMA hydrogels. The UPLC system consisted of Acquity Quaternary Solvent Manager, Sample Manager-FTN, Column Manager, and TUV Detector (Waters Corporation, Milford, MA, USA). Hydrogel samples (6 mm diameter × 2 mm thick) modified or not with CHX-loaded nanotubes were individually immersed into 5 mL DPBS containing 1 U/mL of collagenase type I, followed by incubation at 37 °C. At predetermined time intervals, 500 μL aliquots were drawn, and the same amounts were added back to maintain the extraction volume constant. The aliquots were filtered using a 0.22 μm nylon membrane under vacuum prior to analysis. Separation of the CHX was carried out with an Acquity UPLC-BEH C18 column (1.7 μm, 2.1 × 100 mm) at 40 °C. The mobile phase was acetonitrile/buffer (1% triethylamine adjusted to pH 3.5 by acetic acid)/(35/65) at 0.5 mL/min with an injection volume of 10 μL. CHX concentration was detected by UV absorbance at 259 nm.

Swelling and Enzymatic Degradation.

The swelling capacity of the GelMA-based hydrogels was determined by using the known hydration of the gels. Briefly, after incubation in DPBS at 37 °C for 24 h, wet samples (6 mm diameter × 2 mm thick, n = 3/group) were blot-dried using low-lint content tissue paper (Kimberly-Clark, Irving, TX, USA) and weighed on an analytical balance to obtain wet weights (W_w). The dry weights (W_d) were determined after sample lyophilization. The swelling rate (%) was calculated as $(W_w - W_d)/W_d \times 100$.[22]

For degradation analysis, identical cylindrical-shaped samples (n = 4/group) were incubated in glass vials (VWR International, LLC, Radnor, PA, USA) with 5 mL DPBS containing 1 U/mL collagenase type I at 37 °C. At predetermined time intervals up to 21 days, each

sample was removed from the solution and washed (2×) with sterile DI water, blot-dried, and weighed on an analytical balance. The collagenase-enriched solutions were replaced with fresh ones every 3 days to maintain the constant enzyme activity. The degradation ratio of the hydrogel was calculated using the following equation:

$$\text{Degradation ratio}\,(\%) = \frac{W_t}{W_0} \times 100$$

where W_t is the residual wet weight at different time points, and W_0 is the initial wet weight.

Biomechanical Testing.

To evaluate the compressive modulus, cylindrical-shaped (8 mm diameter × 3 mm thick) samples were prepared. In detail, 150 μL of the GelMA-based hydrogels was dispensed into the mold followed by 15 s of photocross-linking. The samples (n = 5/group) were incubated in DPBS at 37 °C. After 24 h, the samples were blot-dried and then subjected to unconfined compression at a strain rate of 2 mm/min (expert 5601, ADMET Inc., Norwood, MA, USA) at room temperature. The compressive modulus was calculated as the slope of the linear region of the stress-strain curves corresponding with 0–10% strain.[24]

Cytotoxicity.

To examine whether modification of GelMA with CHX-loaded nanotubes would lead to cell toxicity, samples (6 mm diameter × 2 mm thick) were prepared for an *in vitro* assay, in accordance with the International Standards Organization guidelines (ISO10993–5: tests for cytotoxicity-*in vitro* methods). To this end, the samples (n = 5/group) were first UV-treated for 30 min on each side for disinfection purposes and then individually placed in sterile glass vials containing 5 mL of α-MEM supplemented with 10% FBS, L-glutamine, 1% penicillin-streptomycin, and 1 U/mL of collagenase type I. Next, the samples were incubated at 37 °C at predetermined time points up to 28 days, and 500 μL aliquots were collected to determine the cytotoxicity over time. Of note, equal amounts were added back to each vial to keep the extraction volume constant. Finally, the collected aliquots were filtered through a 0.22 μm membrane prior to cell exposure.

SHEDs, kindly donated by Dr. Jacques Nör (University of Michigan, School of Dentistry, Ann Arbor, MI, USA), were cultured in an incubator at 37 °C, with 5% CO_2 in α-MEM supplemented with 10% FBS, 1% L-glutamine, and 1% penicillin-streptomycin.[53] Cells at passages 4–7 were used. SHEDs were seeded at a density of 2.5×10^3 cells/well and allowed to adhere to the wells of 96-well plates. After 24 h, the media was replaced by the collected extracts (100 μL) from the hydrogels and kept in contact with the cells for 24 h. Subsequently, 20 μL of CellTiter 96 AQueous One Solution Reagent was added to the test wells and allowed to react for 2 h at 37 °C in a humidified 5% CO_2 atmosphere. The incorporated dye was measured by reading the absorbance at 490 nm (SpectraMax iD3, Molecular Devices, LLC, San Jose, CA, USA) against a blank column. SHEDs cultured in complete α-MEM were used as a positive control. Absorbance values were converted to a percentage and compared with the values obtained for the test groups.

Determination of Antimicrobial Activities.

The antimicrobial properties of CHX-loaded nanotube-modified GelMA hydrogels were determined by means of an agar diffusion assay against *Actinomyces naeslundii* (*A. naeslundii*, ATCC 12104), *C. albicans* (ATCC 90028), *Fusobacterium nucleatum* (*F. nucleatum*, ATCC 25586), and *E. faecalis* (ATCC 19433). Cylindrical-shaped (6 mm diameter × 2 mm thick) samples were prepared and then disinfected as previously mentioned. The microorganisms were cultured for 24 h in 5 mL of BHI broth. Each bacterial suspension was spectrophotometrically adjusted to obtain 3×10^8 CFU/mL. Each broth (100 μL) was swabbed onto BHI agar plates to form a bacterial lawn.

To determine the sustained antimicrobial effects, and more importantly, the MMP-responsive on-demand nature of the hydrogels, samples (6 mm diameter × 2 mm thick) were prepared (n = 3/group). Next, the samples were individually incubated in glass vials with 5 mL of sterile PBS (with and without 1 U/mL of collagenase type I) at 37 °C. At predetermined time intervals up to 21 days, 500 μL aliquots were drawn and replaced with an equivalent amount of fresh PBS. The retrieved aliquots were stored at −20 °C until further use. Each bacterial plate was divided into four zones, namely 10 μL of 2% chlorhexidine digluconate (CHX; positive control), 10 μL of DI water (negative control), and 20 μL of the GelMA-based aliquots (2 zones/plate randomly assigned). After 24 h (*E. faecalis* and *C. albicans*) or 48 h (*F. nucleatum* and *A. naeslundii*) of incubation, the diameters (in mm) of the clear zones of growth inhibition were measured.

Direct Contact Test.

The direct contact test was performed to investigate the antimicrobial effects of the CHX-loaded nanotube-modified hydrogels in a planktonic model.[54] Samples (6 mm diameter × 2 mm thick) were disinfected by UV-irradiation and then placed on the wells of 96-well plates (n = 6/group). *E. faecalis* was grown overnight in BHI broth in aerobic conditions at 37 °C. of the bacterial suspension (20 μL, 3×10^8 CFU/mL) was added to each well. The samples were incubated for 1 and 24 h at 37 °C. The same volume of bacterial suspension without test samples was also incubated as a control (bacterial growth). After 1 h or 24 h, 180 μL of BHI was added in each well and soaked for 10 min. Each well (100 μL) was transferred to centrifuge tubes containing 900 μL of saline solution for serial dilution. The serial dilutions were carried out in BHI agar plates. Each plate received 3 × 20 μL drops per dilution. The plates were incubated at 37 °C for 24 h and CFU/mL counted.

Microcosm Biofilm.

To determine the antibiofilm properties, the hydrogels that displayed a good relationship between cell viability and antimicrobial activity (over time assays) were selected for testing. Thirty-six recently extracted and caries-free single-root human teeth collected based on a local (University of Michigan, Ann Arbor, MI, USA) Institutional Review Board (HUM-00154490) were cleaned and stored in 0.1% thymol.[55] The teeth were cut to obtain 2 mm thick dentin slices. Briefly, the crowns were sectioned 2 mm above the cementum enamel junction, and a cut was then performed along the buccolingual plane. The specimens were wet-finished with SiC papers (600–1200 grit). The dentin slices were immersed in 2.5% NaOCl and 17% EDTA solutions for 3 min each in an ultrasonic bath, rinsed in sterile

saline solution for 10 min, and then autoclaved at 121 °C for 20 min.[56] A supragingival plaque was collected from a healthy adult volunteer based on a local Institutional Review Board (HUM-00164678) and suspended in BHI broth. This suspension was incubated in an anaerobic chamber for 24 h. Then, the bacterial cell amount was adjusted to ~7.5×10^7 CFU/mL in BHI broth.

The dentin slices were allocated in 24-well plates containing 1.8 mL of BHI and 0.2 mL of the inoculum and then incubated in an anaerobic chamber for 7 days to allow for biofilm formation. The broth was changed every 2 days. Infected dentin slices ($n = 6$/group) were randomly divided into six groups: GelMA, 5%H, 5%H-C10%, 5%H-C20%, $Ca(OH)_2$ paste (positive control), and an untreated 7-day-old biofilm (negative control). After 7 days, the nonadherent bacteria were removed from the samples by gently rinsing them in PBS. Then, 50 μL of each hydrogel formulation was placed above the biofilm/dentin samples and photocross-linked for 15 s. The samples were incubated for 7 days in the anaerobic chamber. Next, the samples were allocated to determine CFU/mL ($n = 4$) and for SEM imaging ($n = 2$).

For CFU/mL, the samples were carefully removed from the wells and placed in centrifuge tubes containing 1000 μL of saline solution for serial dilution. The dilutions were carried out in BHI agar plates. The plates were incubated at 37 °C for 24 h in an anaerobic chamber, and the CFU/mL was counted. For SEM evaluation, the samples were removed from the wells, gently washed in PBS, and fixed overnight in 2.5% glutaraldehyde. The samples were then dehydrated in increasing concentrations of alcohol solution. After dehydration, the samples were placed in increasing concentrations of HMDS solutions. The dentin slices were then coated with Au-Pd prior to SEM imaging.[56]

In Vivo Biocompatibility and Biodegradation.

All animal procedures followed the ARRIVE guidelines for reporting animal research and were in accordance with the procedures of the local Institutional Animal Care and Use Committee (PRO00008502). Eight 6-week-old male Fischer 344 rats (300–320 g) were allocated for the experiments (Envigo RMS, Inc., Oxford, MI, USA). All surgical procedures were performed under general anesthesia induced with inhalation isoflurane (Piramal, PA, USA) (4–5%) for induction and maintained with isoflurane (1–3%). After anesthesia, small separated subcutaneous pockets were bluntly created through short dorsal skin incisions (10 mm in length), and cylindrical-shaped samples (8 mm diameter × 3 mm thick) of GelMA, 5%H and 5%H-C10% hydrogels were implanted ($n = 4$/group). Sham was used as a control. After wound closure, the animals were allowed to recover from anesthesia. At 7- or 14-days postimplantation, the animals were euthanized by CO_2 inhalation, and the implanted hydrogels were retrieved together with the surrounding peri-implantation tissue and fixed in 10% buffered formalin overnight. The fixed explanted samples were then embedded in paraffin, cut in 6 μm-thick sections, and stained with H&E to investigate under light microscopy for the presence of luminal structures containing red blood and inflammatory cells while also assessing hydrogel degradation (Nikon E800, Shinagawa, Tokyo, Japan).[44]

Statistics.

Statistical analysis was performed by one-way analysis of variance, and a *p*-value of less than 0.05 was considered to be statistically significant.

ACKNOWLEDGMENTS

M.C.B. acknowledges the National Institutes of Health (NIH, National Institute of Dental and Craniofacial Research/NIDCR) (Grants K08DE023552 and R01DE026578). The content is solely the responsibility of the authors and does not necessarily represent the official views of the National Institutes of Health. J.S.R. was supported in part by a scholarship from CAPES Foundation (Brazil).

REFERENCES

(1). National Center for Health Statistics. NCHS Data Brief, Number 307, 7 2018, 2015–2016, https://www.cdc.gov/nchs/data/databriefs/db307_table.pdf#1.

(2). Eramo S; Natali A; Pinna R; Milia E Dental Pulp regeneration via Cell Homing. Int. Endod. J 2018, 51, 405–419. [PubMed: 29047120]

(3). Eklund SA Trends in Dental Treatment, 1992 to 2007. J. Am. Dent. Assoc 2010, 141, 391–399. [PubMed: 20354088]

(4). Qian W; Ma T; Ye M; Li Z; Liu Y; Hao P Microbiota in the Apical Root Canal System of Tooth with Apical Periodontitis. BMC Genomics 2019, 20, 189. [PubMed: 30967114]

(5). Antunes HS; Rôças IN; Alves FRF; Siqueira JF Total and Specific Bacterial Levels in the Apical Root Canal System of Teeth with Post-treatment Apical Periodontitis. J. Endod 2015, 41, 1037–1042. [PubMed: 25892512]

(6). Narayanan L; Vaishnavi C Endodontic Microbiology. J. Conservative Dent 2010, 13, 233–239.

(7). Harrington DJ Bacterial Collagenases and Collagen-degrading Enzymes and their Potential Role in Human Disease. Infect. Immun 1996, 64, 1885–1891. [PubMed: 8675283]

(8). Sorsa T; Ingman T; Suomalainen K; Haapasalo M; Konttinen YT; Lindy O; Saari H; Uitto VJ Identification of Proteases from Periodontopathogenic Bacteria as Activators of Latent Human Neutrophil and Fibroblast-type Interstitial Collagenases. Infect. Immun 1992, 60, 4491–4495. [PubMed: 1398963]

(9). De-Deus G; Barino B; Zamolyi RQ; Souza E; Fonseca A Jr.; Fidel S; Sergio Fidel RA Suboptimal Debridement Quality Produced by the Single-file F2 Protaper Technique in Oval-shaped Canals. J. Endod 2010, 36, 1897–1900. [PubMed: 20951309]

(10). Gomes BPFA; Vianna ME; Zaia AA; Almeida JFA; Souza-Filho FJ; Ferraz CCR Chlorhexidine in Endodontics. Braz. Dent. J 2013, 24, 89–102. [PubMed: 23780357]

(11). Marwah N; Dutta S; Singla R Single Visit versus Multiple Visit Root Canal Therapy. Int. J. Clin. Pediatr. Dent 2008, 1, 17–24. [PubMed: 25206084]

(12). Mohammadi Z Chlorhexidine Gluconate, its Properties and Applications in Endodontics. Iran. Endod. J 2008, 2, 113–125. [PubMed: 24265633]

(13). Barbosa-Ribeiro M; Arruda-Vasconcelos R; de-Jesus-Soares A; Zaia AA; Ferraz CCR; de Almeida JFA; Gomes BPFA Effectiveness of Calcium Hydroxide-based Intracanal Medication on Infectious/inflammatory Contents in Teeth with Post-treatment Apical Periodontitis. Clin. Oral Invest 2019, 23, 2759–2766.

(14). Pereira MSS; Faria G; Bezerra Da Silva LA; Tanomaru-Filho M; Kuga MC; Rossi MA Response of Mice Connective Tissue to Intracanal Dressings Containing Chlorhexidine. Microsc. Res. Tech 2012, 75, 1653–1658. [PubMed: 22887775]

(15). Lessa FCR; Aranha AMF; Nogueira I; Giro EMA; Hebling J; Costa C. A. d. S. Toxicity of Chlorhexidine on Odontoblast-like Cells. J. Appl. Oral Sci 2010, 18, 50–58. [PubMed: 20379682]

(16). Feitosa SA; Palasuk J; Geraldeli S; Windsor LJ; Bottino MC Physicochemical and Biological Properties of Novel Chlorhexidine-loaded Nanotube-modified Dentin Adhesive. J. Biomed. Mater. Res., Part B 2019, 107, 868–875.

(17). Palasuk J; Windsor LJ; Platt JA; Lvov Y; Geraldeli S; Bottino MC Doxycycline-loaded Nanotube-modified Adhesives Inhibit MMP in a Dose-dependent Fashion. Clin. Oral Invest 2018, 22, 1243–1252.

(18). Abdullayev E; Lvov Y Halloysite Clay Nanotubes as a Ceramic “Skeleton” for Functional Biopolymer Composites with Sustained Drug Release. J. Mater. Chem. B 2013, 1, 2894–2903. [PubMed: 32260855]

(19). Wei W; Minullina R; Abdullayev E; Fakhrullin R; Mills D; Lvov Y Enhanced Efficiency of Antiseptics with Sustained Release from Clay Nanotubes. RSC Adv. 2014, 4, 488–494.

(20). Qi R; Guo R; Shen M; Cao X; Zhang L; Xu J; Yu J; Shi X Electrospun Poly(lactic-co-glycolic acid)/halloysite Nanotube Composite Nanofibers for Drug Encapsulation and Sustained Release. J. Mater. Chem 2010, 20, 10622–10629.

(21). Rahali K; Ben Messaoud G; Kahn CJF; Sanchez-Gonzalez L; Kaci M; Cleymand F; Fleutot S; Linder M; Desobry S; Arab-Tehrany E Synthesis and Characterization of Nanofunctionalized Gelatin Methacrylate Hydrogels. Int. J. Mol. Sci 2017, 18, 2675.

(22). Nichol JW; Koshy ST; Bae H; Hwang CM; Yamanlar S; Khademhosseini A Cell-laden Microengineered Gelatin Methacrylate Hydrogels. Biomaterials 2010, 31, 5536–5544. [PubMed: 20417964]

(23). Monteiro N; Thrivikraman G; Athirasala A; Tahayeri A; França CM; Ferracane JL; Bertassoni LE Photopolymerization of Cell-laden Gelatin Methacryloyl Hydrogels Using a Dental Curing Light for Regenerative Dentistry. Dent. Mater 2018, 34, 389–399. [PubMed: 29199008]

(24). Paul A; Manoharan V; Krafft D; Assmann A; Uquillas JA; Shin SR; Hasan A; Hussain MA; Memic A; Gaharwar AK; Khademhosseini A Nanoengineered Biomimetic Hydrogels for Guiding Human Stem Cell Osteogenesis in Three Dimensional Microenvironments. J. Mater. Chem. B 2016, 4, 3544–3554. [PubMed: 27525102]

(25). Paula-Silva FWG; da Silva LAB; Kapila YL Matrix Metalloproteinase Expression in Teeth with Apical Periodontitis is Differentially Modulated by the Modality of Root Canal Treatment. J. Endod 2010, 36, 231–237. [PubMed: 20113780]

(26). Jain A; Bahuguna R Role of Matrix Metalloproteinases in Dental Caries, Pulp and Periapical Inflammation: An Overview. J. Oral Biol. Craniofac. Res 2015, 5, 212–218. [PubMed: 26605147]

(27). Abdullayev E; Lvov Y Halloysite Clay Nanotubes for Controlled Release of Protective Agents. J. Nanosci. Nanotechnol 2011, 11, 10007–10026. [PubMed: 22413340]

(28). Gupte MJ; Ma PX Nanofibrous Scaffolds for Dental and Craniofacial Applications. J. Dent. Res 2012, 91, 227–234. [PubMed: 21828356]

(29). Zhu Y; Zhang Q; Shi X; Han D Hierarchical Hydrogel Composite Interfaces with Robust Mechanical Properties for Biomedical Applications. Adv. Mater 2019, 31, 1804950.

(30). Raso EMG; Cortes ME; Teixeira KI; Franco MB; Mohallem NDS; Sinisterra RD A New Controlled Release System of Chlorhexidine and Chlorhexidine: βcd Inclusion Compounds Based on Porous Silica. J. Inclusion Phenom. Macrocyclic Chem 2010, 67, 159–168.

(31). Sun J; Iakunkov A; Rebrikova AT; Talyzin AV Exactly Matched Pore Size for the Intercalation of Electrolyte Ions Determined Using the Tunable Swelling of Graphite Oxide in Supercapacitor Electrodes. Nanoscale 2018, 10, 21386–21395. [PubMed: 30427042]

(32). Kirsch M; Birnstein L; Pepelanova I; Handke W; Rach J; Seltsam A; Scheper T; Lavrentieva A Gelatin-Methacryloyl (GelMA) Formulated with Human Platelet Lysate Supports Mesenchymal Stem Cell Proliferation and Differentiation and Enhances the Hydrogel’s Mechanical Properties. Bioengineering 2019, 6, 76.

(33). Huang K; Ou Q; Xie Y; Chen X; Fang Y; Huang C; Wang Y; Gu Z; Wu J Halloysite Nanotube Based Scaffold for Enhanced Bone Regeneration. ACS Biomater. Sci. Eng 2019, 5, 4037–4047.

(34). Modaresifar K; Hadjizadeh A; Niknejad H Design and Fabrication of GelMA/chitosan Nanoparticles Composite Hydrogel for Angiogenic Growth Factor Delivery. Artif. Cells, Nanomed., Biotechnol 2017, 46, 1799–1808. [PubMed: 29065727]

(35). Pepelanova I; Kruppa K; Scheper T; Lavrentieva A Gelatin-Methacryloyl (GelMA) Hydrogels with Defined Degree of Functionalization as a Versatile Toolkit for 3D Cell Culture and Extrusion Bioprinting. Bioengineering 2018, 5, 55.

(36). Kayaoglu G; Ørstavik D Virulence Factors of Enterococcus faecalis: Relationship to Endodontic Disease. Crit. Rev. Oral Biol. Med 2004, 15, 308–320. [PubMed: 15470268]

(37). Neelakantan P; Romero M; Vera J; Daood U; Khan AU; Yan A; Cheung GSP. Biofilms in Endodontics-Current Status and Future Directions. Int. J. Mol. Sci 2017, 18, 1748.

(38). Devaraj S; Jagannathan N; Neelakantan P Antibiofilm Efficacy of Photoactivated Curcumin, Triple and Double Antibiotic Paste, 2% Chlorhexidine and Calcium Hydroxide Against Enterococcus faecalis In Vitro. Sci. Rep 2016, 6, 24797. [PubMed: 27097667]

(39). Stuart C; Schwartz S; Beeson T; Owatz C Enterococcus faecalis: Its Role in Root Canal Treatment Failure and Current Concepts in Retreatment. J. Endod 2006, 32, 93–98. [PubMed: 16427453]

(40). Sjögren U; Figdor D; Spångberg L; Sundqvist G The Antimicrobial Effect of Calcium Hydroxide as a Short-term Intracanal Dressing. Int. Endod. J 1991, 24, 119–125. [PubMed: 1778624]

(41). Segura-Egea JJ; Gould K; Sen BH; Jonasson P; Cotti E; Mazzoni A; Sunay H; Tj äderhane L; Dummer PMH European Society of Endodontology Position Statement: The Use of Antibiotics in Endodontics. Int. Endod. J 2018, 51, 20–25. [PubMed: 28436043]

(42). Yang G; Xiao Z; Long H; Ma K; Zhang J; Ren X; Zhang J Assessment of the Characteristics and Biocompatibility of Gelatin Sponge Scaffolds Prepared by Various Crosslinking Methods. Sci. Rep 2018, 8, 1616. [PubMed: 29371676]

(43). Assmann A; Vegh A; Ghasemi-Rad M; Bagherifard S; Cheng G; Sani ES; Ruiz-Esparza GU; Noshadi I; Lassaletta AD; Gangadharan S; Tamayol A; Khademhosseini A; Annabi N A Highly Adhesive and Naturally Derived Sealant. Biomaterials 2017, 140, 115–127. [PubMed: 28646685]

(44). Chen Y-C; Lin R-Z; Qi H; Yang Y; Bae H; Melero-Martin JM; Khademhosseini A Functional Human Vascular Network Generated in Photocrosslinkable Gelatin Methacrylate Hydrogels. Adv. Funct. Mater 2012, 22, 2027–2039. [PubMed: 22907987]

(45). Labow RS; Tang Y; McCloskey CB; Santerre JP The Effect of Oxidation on the Enzyme-catalyzed Hydrolytic Biodegradation of Poly(urethane)s. J. Biomater. Sci., Polym. Ed 2002, 13, 651–665. [PubMed: 12182550]

(46). McBane JE; Santerre JP; Labow RS Role of Protein Kinase C in the Monocyte-derived Macrophage-mediated Biodegradation of Polycarbonate-based Polyurethanes. J. Biomed. Mater. Res., Part A 2005, 74A, 1–11.

(47). McBane JE; Santerre JP; Labow R Effect of Phorbol Esters on the Macrophage-mediated Biodegradation of Polyurethanes via Protein Kinase C Activation and other Pathways. J. Biomater. Sci., Polym. Ed 2009, 20, 437–453. [PubMed: 19228446]

(48). Annabi N; Rana D; Shirzaei Sani E; Portillo-Lara R; Gifford JL; Fares MM; Mithieux SM; Weiss AS Engineering a Sprayable and Elastic Hydrogel Adhesive with Antimicrobial Properties for Wound Healing. Biomaterials 2017, 139, 229–243. [PubMed: 28579065]

(49). Sambandam V; Neelakantan P Matrix Metalloproteinases (mmp) in Restorative Dentistry and Endodontics. J. Clin. Pediatr. Dent 2014, 39, 57–59. [PubMed: 25631728]

(50). Sakko M; Tjäderhane L; Rautemaa-Richardson R Microbiology of Root Canal Infections. Prim. Dent. J 2016, 5, 84–89. [PubMed: 28826437]

(51). Xiao W; He J; Nichol JW; Wang L; Hutson CB; Wang B; Du Y; Fan H; Khademhosseini A Synthesis and Characterization of Photocrosslinkable Gelatin and Silk Fibroin Interpenetrating Polymer Network Hydrogels. Acta Biomater. 2011, 7, 2384–2393. [PubMed: 21295165]

(52). Van Den Bulcke AI; Bogdanov B; De Rooze N; Schacht EH; Cornelissen M; Berghmans H Structural and Rheological Properties of Methacrylamide Modified Gelatin Hydrogels. Biomacromolecules 2000, 1, 31–38. [PubMed: 11709840]

(53). Rosa V; Zhang Z; Grande RHM; Nör JE Dental Pulp Tissue Engineering in Full-length Human Root Canals. J. Dent. Res 2013, 92, 970–975. [PubMed: 24056227]

(54). Correa CF; Santana LR; Silva RM; Noremberg BS; Lund RG; Ribeiro JS; Motta FV; Bomio MRD; Nascimento RM; Carreño NLV Antimicrobial Activity from Polymeric Composites-based Polydimethylsiloxane/TiO2/GO: Evaluation of Filler Synthesis and Surface Morphology. Polym. Bull 2017, 74, 2379–2390.

(55). Bottino MC; Albuquerque MTP; Azabi A; Münchow EA; Spolnik KJ; Nör JE; Edwards PC A Novel Patient-specific Three-dimensional Drug Delivery Construct for Regenerative Endodontics. J. Biomed. Mater. Res., Part B 2019, 107, 1576–1586.

(56). Albuquerque MTP; Valera MC; Moreira CS; Bresciani E; de Melo RM; Bottino MC Effects of Ciprofloxacin-containing Scaffolds on Enterococcus faecalis Biofilms. J. Endod 2015, 41, 710–714. [PubMed: 25698261]

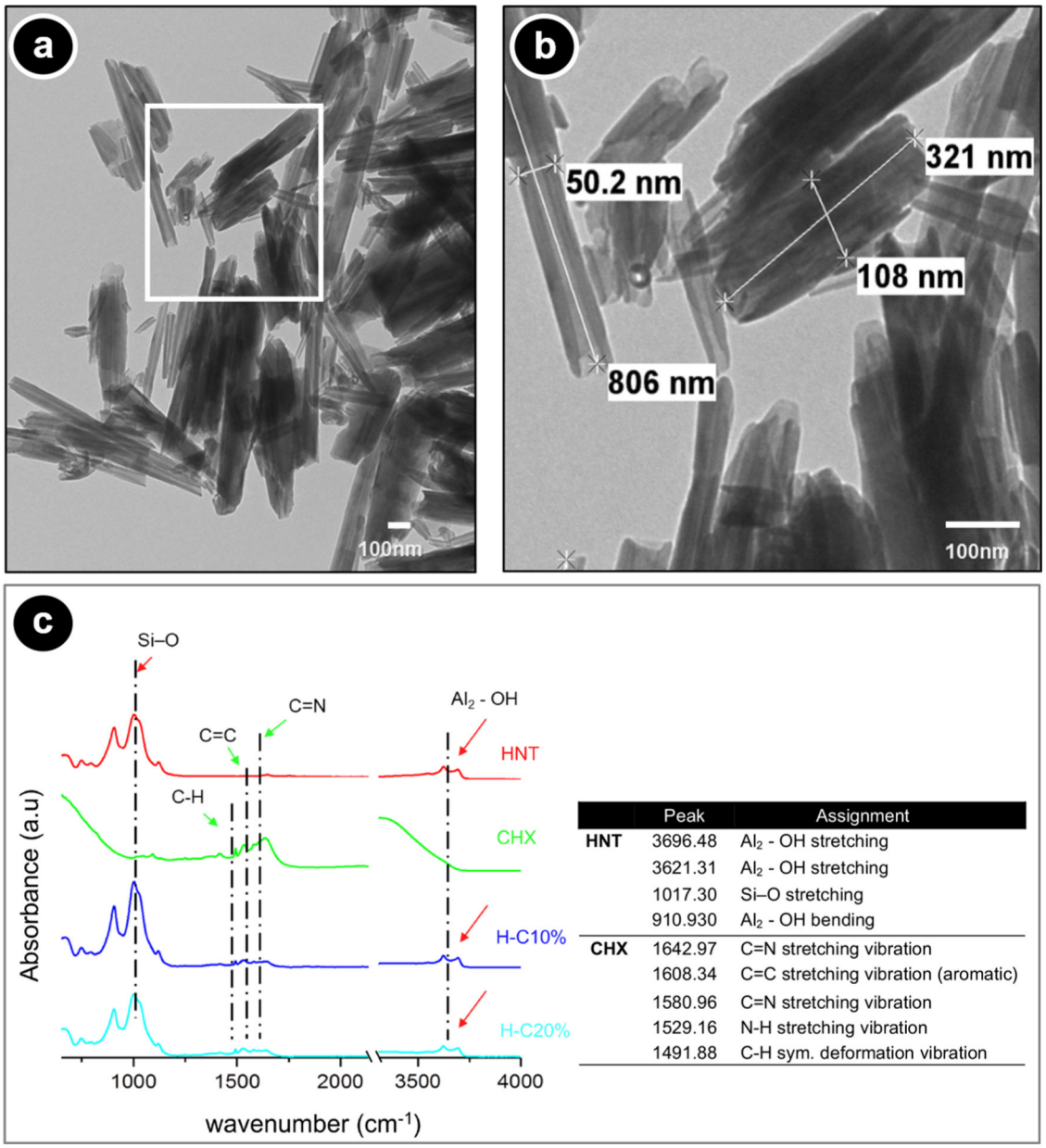

	Peak	Assignment
HNT	3696.48	Al_2 - OH stretching
	3621.31	Al_2 - OH stretching
	1017.30	Si–O stretching
	910.930	Al_2 - OH bending
CHX	1642.97	C=N stretching vibration
	1608.34	C=C stretching vibration (aromatic)
	1580.96	C=N stretching vibration
	1529.16	N-H stretching vibration
	1491.88	C-H sym. deformation vibration

Figure 1.

Morphological and chemical analyses of the nanotubes (HNTs, Halloysite, Dragonite HP) with and without CHX. (a) Representative TEM micrograph of the as-received HNTs. (b) Inset high-magnification TEM micrograph showing the uniform rod-like tubular structure, the hollow nature, and the morphological aspect of the tubes (scale bar = 100 nm). (c) ATR-FTIR spectra for pristine HNTs, CHX, and CHX-loaded nanotubes.

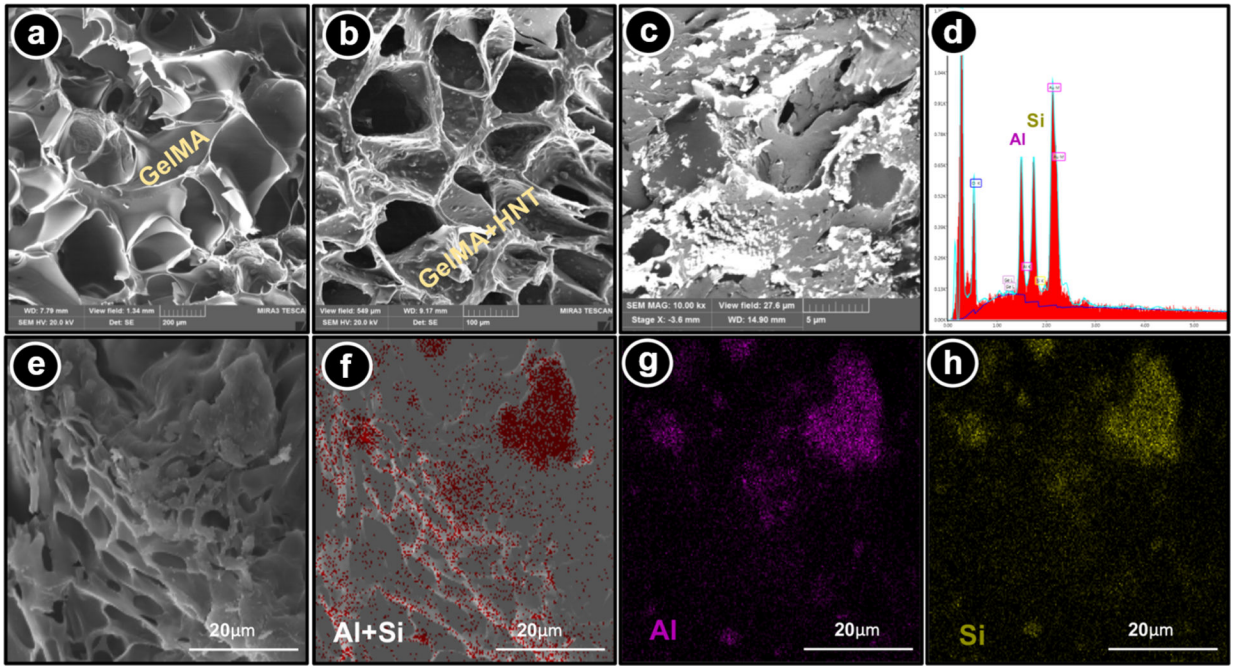

Figure 2.

Morphological and chemical analyses of the nanotube-modified GelMA-based hydrogels. (a) SEM micrograph of a GelMA hydrogel cross-section. (b) SEM and (c) BSE-SEM micrographs of a cross-section of GelMA modified with CHX-loaded nanotubes (5% H-10% C). Note the presence of the aluminosilicate nanotubes based on the brightest areas throughout the microstructure (⧫). (d) EDS results confirm the presence of Si and Al. (e-h) SEM micrographs combined with BSE-EDS elemental mapping of cross-section GelMA hydrogel modified with CHX-loaded nanotubes show a uniform distribution of the nanotubes within the hydrogel matrix.

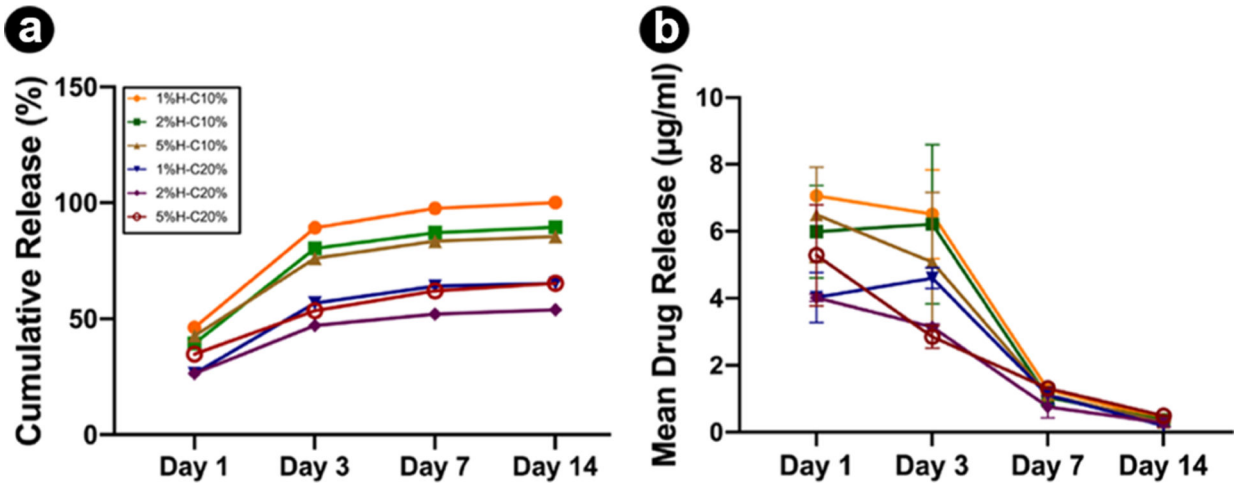

Figure 3.

In vitro CHX release profiles from nanotube-modified GelMA loaded with distinct nanotube (1, 2, and 5%) concentration and CHX solution concentration (10 and 20%) as a function of time. (a) Cumulative release (in %) and (b) mean drug release (in μg/mL). The results are presented as mean ± standard deviation (SD) (n = 4).

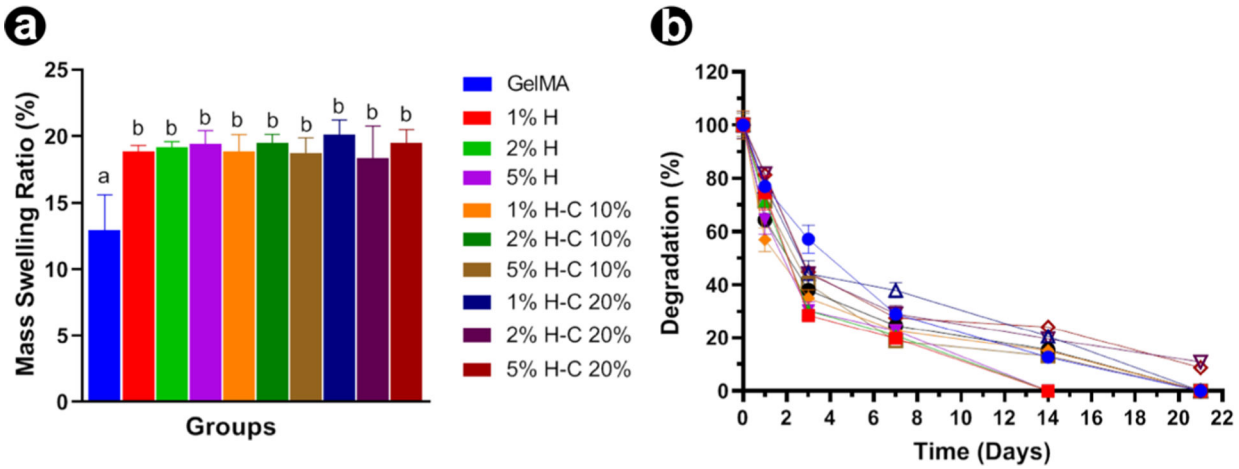

Figure 4.

Swelling and enzymatic degradation (mass loss) of GelMA-based hydrogels. (a) Swelling ratio of GelMA and nanotube-modified GelMA-based hydrogels with and without CHX loading in DPBS at 37 °C. (b) *In vitro* biodegradation of GelMA and nanotube-modified hydrogels in DPBS containing 1 U/mL of collagenase type I at 37 °C. The results are presented as mean ± SD ($n = 4$).

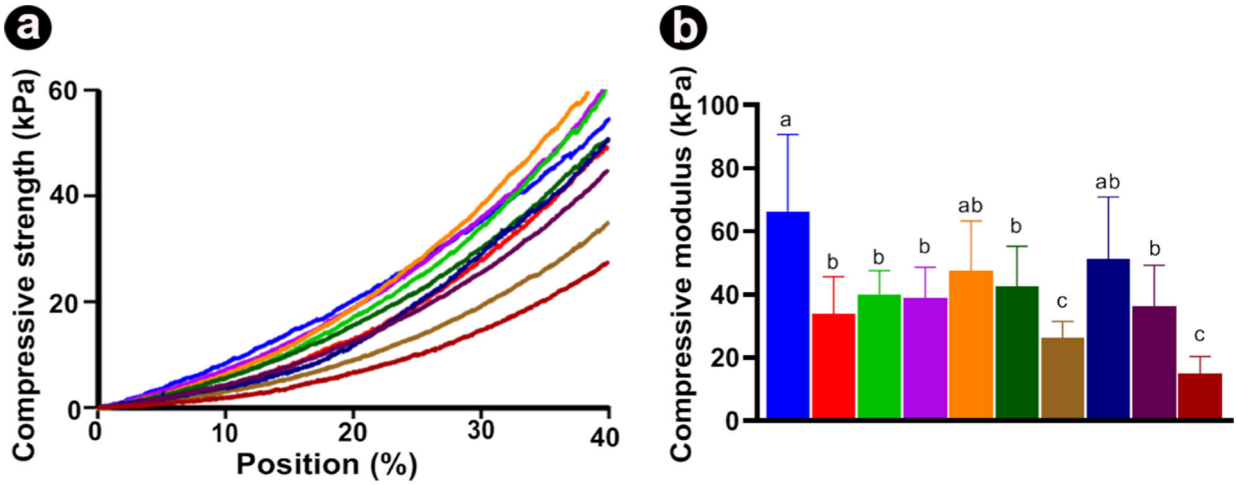

Figure 5.

Biomechanical properties of GelMA-based hydrogels. (A) Representative stress-strain curves from nanotube-modified GelMA hydrogels loaded with different concentrations of nanotubes (1, 2, and 5%) and chlorhexidine solution concentration (CHX at 10 and 20%). (B) Compressive modulus (in kPa). The results are presented as mean ± SD (n = 10).

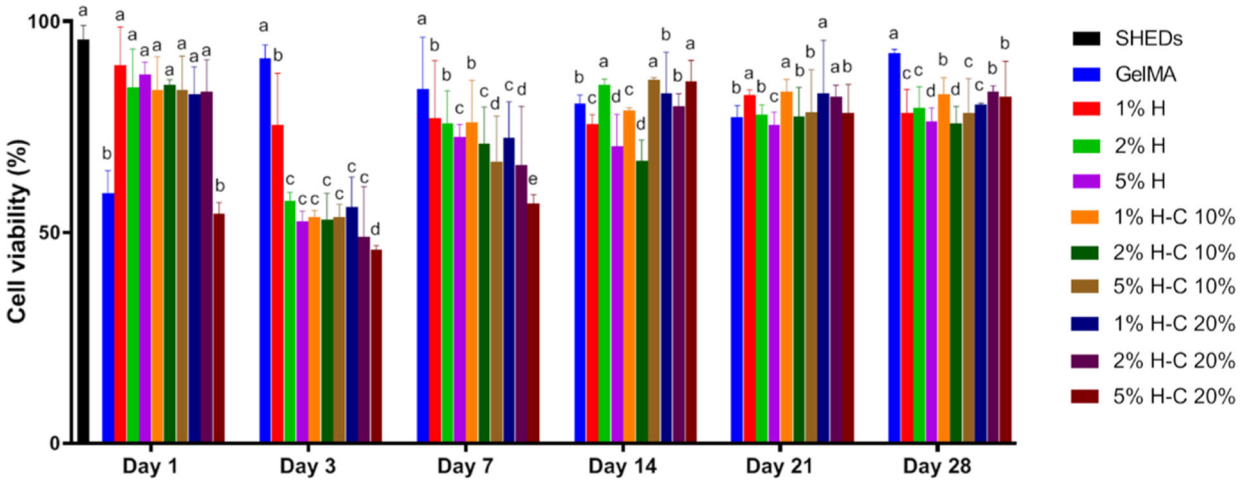

Figure 6.

Cytotoxicity assay measured viability (%) of SHEDs in response to aliquots at day 1, 3, 7, 14, 21, and 28 from GelMA-based hydrogels modified or not with 1, 2, and 5% of halloysite nanotubes (H) and CHX-loaded nanotubes (H-C10% and H-C20%). Statistical analyses were compared with the same day. The percentage of cell viability was normalized by the mean absorbance of SHEDs cultured in the plate at day 1 (100%). Distinct letters indicate statistically significant differences between the groups when compared with the control (SHED cells). The results are presented as mean ± SD ($n = 5$).

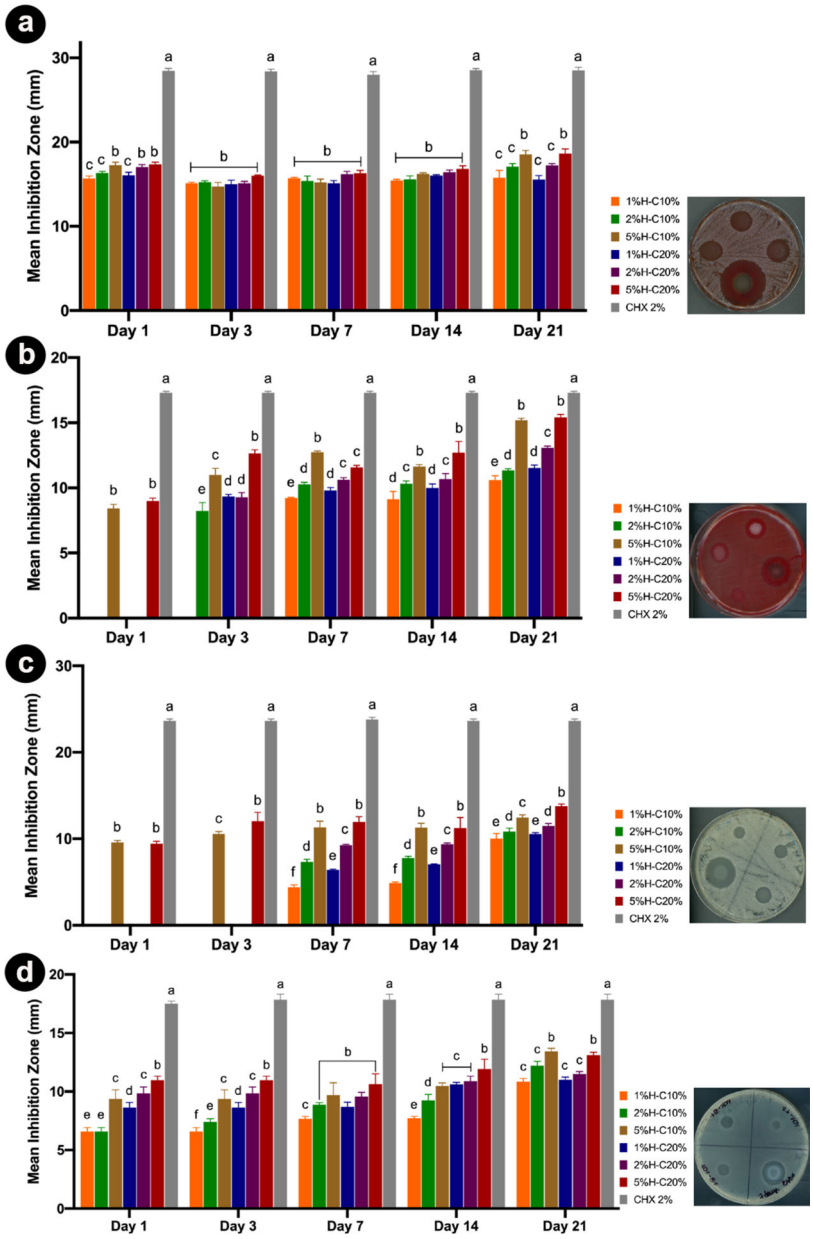

Figure 7.

Results from the agar diffusion assays are represented as a mean inhibition zone (in mm) against the different pathogens tested. (a) *A. naeslundii*; (b) *F. nucleatum*; (c) *C. albicans*, and (d) *E. faecalis* over time. Aliquots obtained through incubation in PBS only and incubated at the on-demand challenge (1 U/mL collagenase type A), over 21 days, were tested. The same letters indicate an insignificant difference compared to the results of the same day of aliquots.

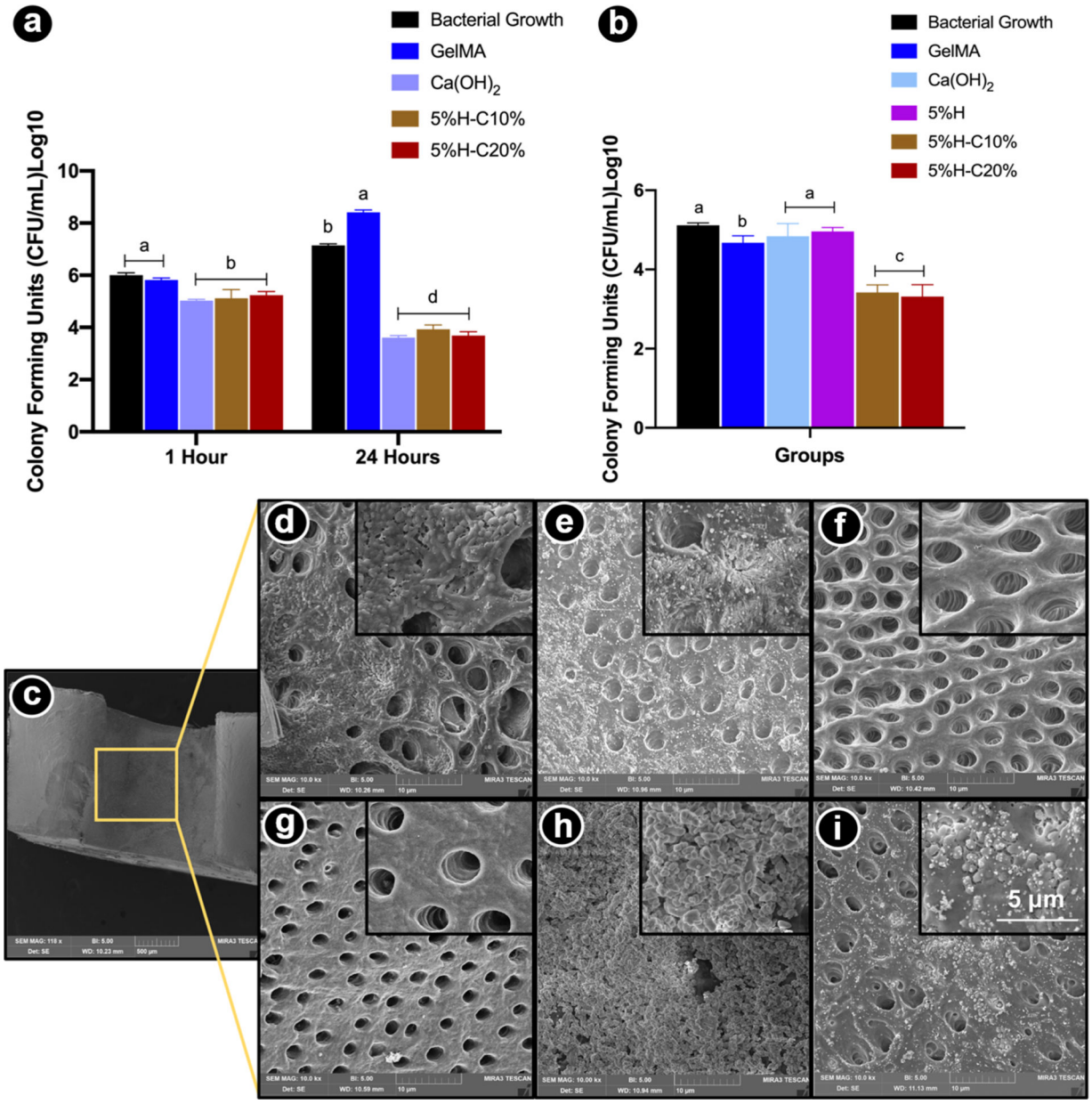

Figure 8.

Antimicrobial properties of the formulated hydrogels. (a) Modified direct contact assay. Mean counts of viable (CFU/mL) planktonic bacterial cells on GelMA-modified hydrogels. (b) Microcosm biofilm model. CHX-loaded GelMA-based hydrogels (5%H-C10% and 5%H-C20%) significantly reduced bacterial numbers compared to all other groups. (c) SEM micrograph depicting the evaluated areas (inner root walls of dentin slices). (d-i) SEM micrographs of bacterial biofilm on the dentin surface of pristine GelMA (d), GelMA-5%H (e), GelMA-5%H-10%C (f), GelMA-5%H-20%C (g), $Ca(OH)_2$ (h), and bacterial growth, that is, untreated dentin (i). Unmodified GelMA, CHX-free nanotube-modified GelMA groups demonstrate bacteria on dentin surfaces and inside dentinal tubules. CHX-loaded nanotube-modified GelMA hydrogels eliminated almost all bacteria on the dentin surface

and inside dentinal tubules. Infected dentin slices treated with $Ca(OH)_2$ show bacterial presence within the calcium hydroxide paste. Note the abundant presence of biofilm on untreated dentin surfaces.

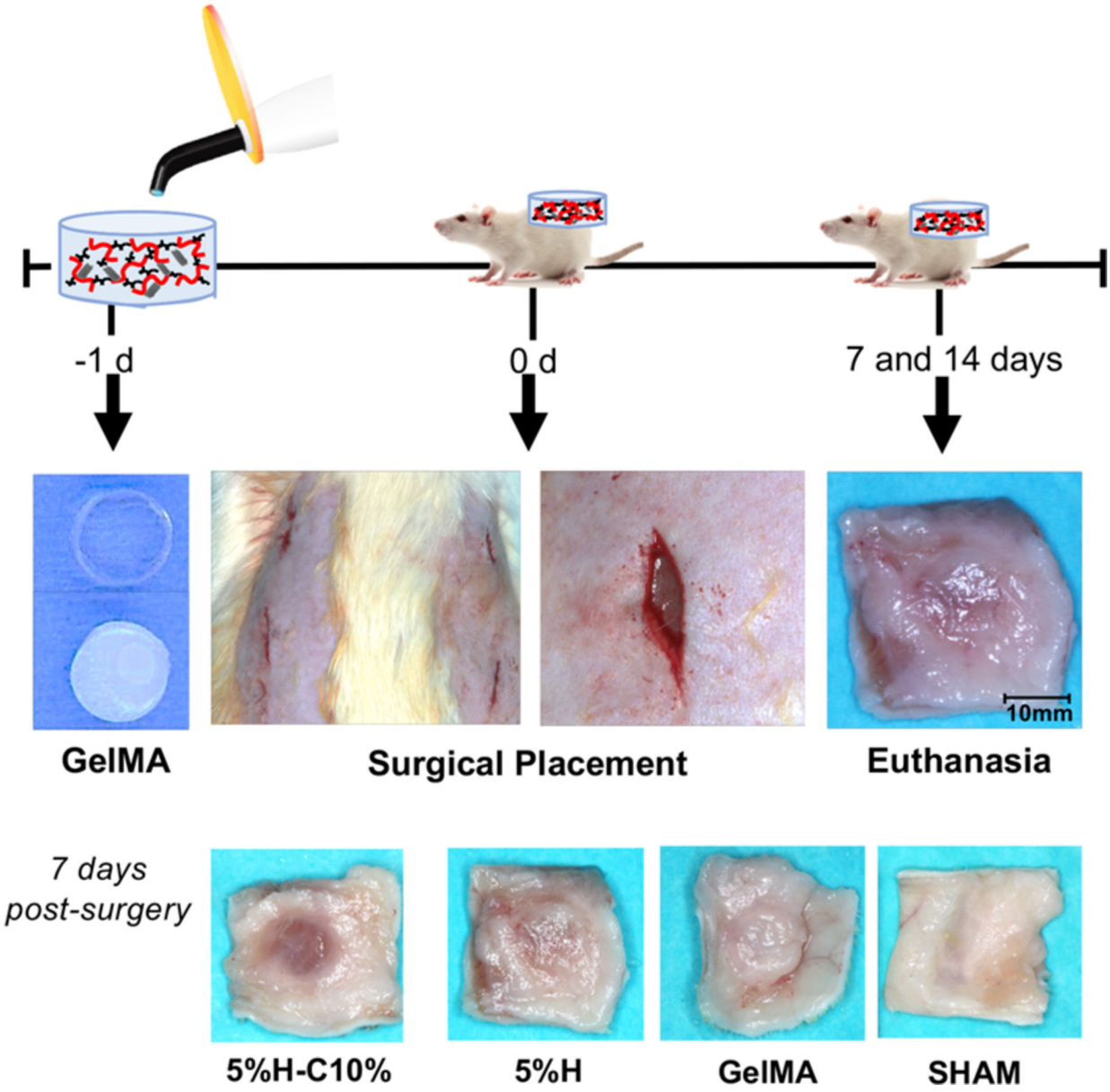

Figure 9.

In vivo biocompatibility and biodegradation of the GelMA-based hydrogels. Schematic representation of the surgical implantation of GelMA, 5%H, and 5%H-C10% hydrogels in a dorsal subcutaneous region of 6-week old Fischer 344 rats. The hydrogel samples were retrieved after 7 and 14 days. Representative macrophotographs of the explants' 7 day postimplantation.

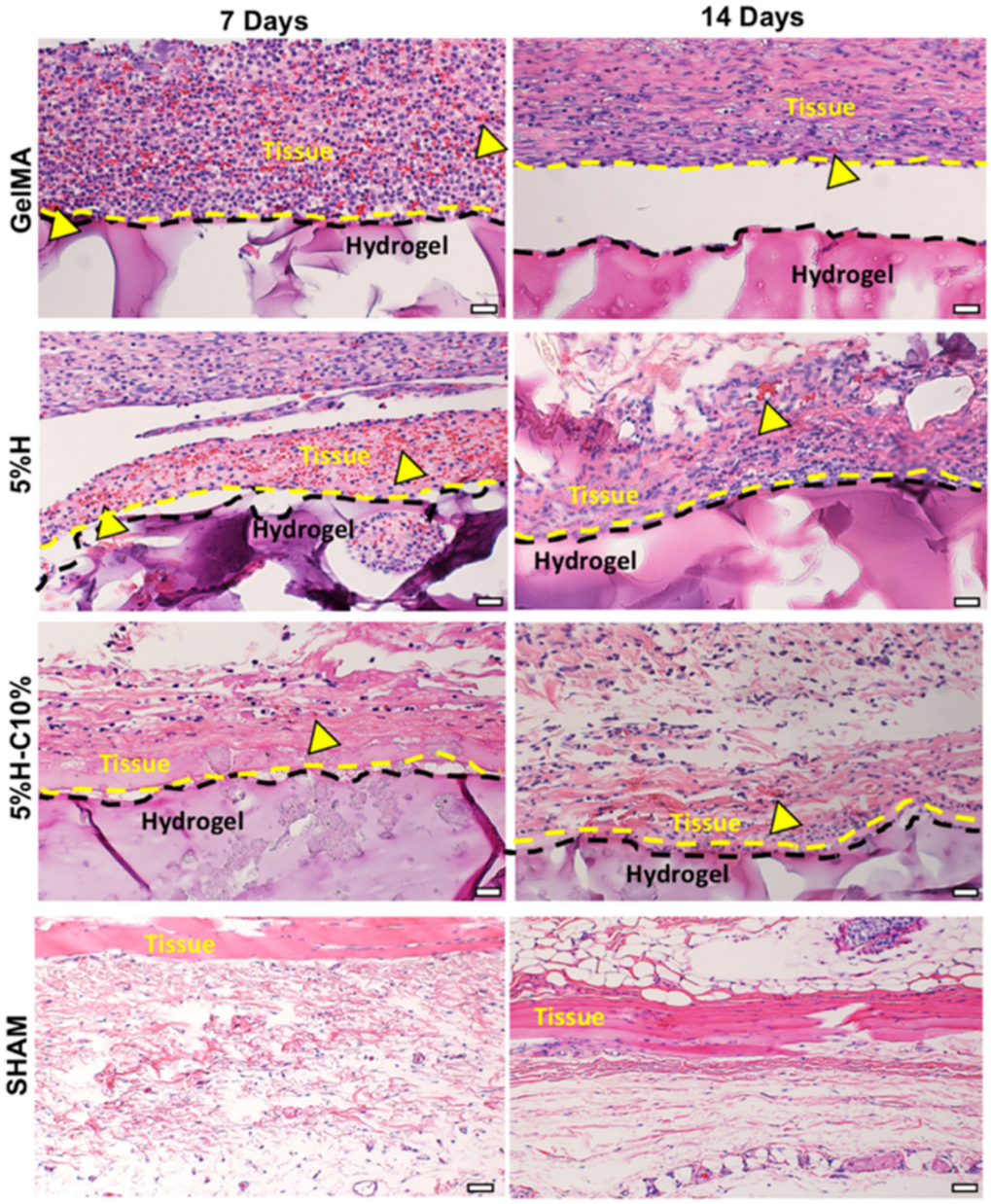

Figure 10.

Histological analysis of the implanted hydrogels. Representative H&E staining images of GelMA, 5%H, 5%H-C10%, and SHAM explants (hydrogels with the surrounding tissue) after 7 and 14 days *in vivo* (scale bar = 200 μm). Yellow arrowheads indicate the presence of numerous blood vessels containing murine erythrocytes.

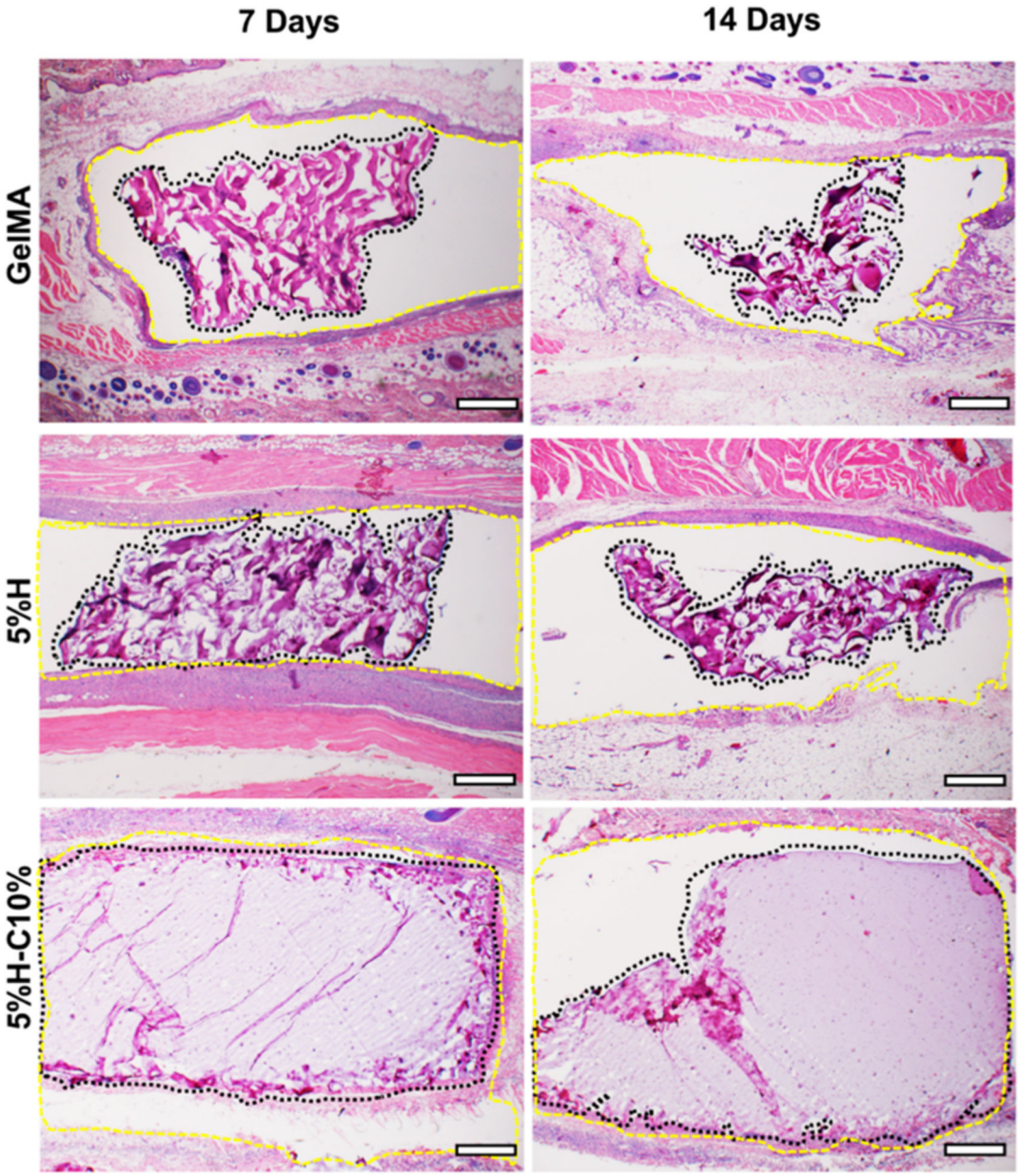

Figure 11.

Histological analysis of the implanted GelMA hydrogels. Representative H&E staining images of GelMA, 5%H, 5%H-C10%, and SHAM explants (hydrogels with the surrounding tissue) after 7 and 14 days *in vivo* (scale bar = 200 μm). The black dashed lines delineate the implanted hydrogel border, highlighting the hydrogel degradation over time while the yellow dashed lines delineate the subcutaneous tissue surrounding the hydrogel.